Radiology

ORIGINAL RESEARCH • CARDIAC IMAGING

Circumferential Strain Predicts Major Adverse Cardiovascular Events Following an Acute ST-Segment–Elevation Myocardial Infarction

Kenneth Mangion, MD • David Carrick, PhD • Jaclyn Carberry, MBChB • Ahmed Mahrous, MD • Christie McComb, PhD • Keith G. Oldroyd, MD • Hany Eteiba, MD • Mitchell Lindsay, MD • Margaret McEntegart, PhD • Stuart Hood, MD • Mark C. Petrie, MBChB • Stuart Watkins, MD • Andrew Davie, MBChB • Xiaodong Zhong, PhD • Frederick H. Epstein, PhD • Caroline E. Haig, PhD • Colin Berry, PhD

From the British Heart Foundation Glasgow Cardiovascular Research Centre, Institute of Cardiovascular and Medical Sciences (K.M., D.C., J.C., C.M., M.C.P., C.B.), and Robertson Centre for Biostatistics (C.E.H.), University of Glasgow, 126 University Place, Glasgow G12 8TA, Scotland; West of Scotland Heart and Lung Centre, Golden Jubilee National Hospital, Clydebank, Scotland (K.M., D.C., A.M., K.G.O., H.E., M.L., M.M., S.H., M.C.P., S.W., A.D., C.B.); Department of Clinical Physics, NHS Greater Glasgow and Clyde, Glasgow, Scotland (C.M.); Department of MR R&D Collaborations, Siemens Healthcare, Atlanta, Ga (X.Z.); and Department of Biomedical Engineering, University of Virginia, Charlottesville, Va (F.H.E.). Received May 26, 2018; revision requested July 16; final revision received September 16; accepted September 20. **Address correspondence to** C.B. (e-mail: *colin.berry@glasgow.ac.uk*).

K.M. supported by a fellowship from the British Heart Foundation (FS/15/54/31639). C.B. supported by a senior clinical fellowship from the Scottish Funding Council and the British Heart Foundation Centre of Excellence Award (RE/13/5/3017). Supported by project grants from the Chief Scientist Office (SC01), Medical Research Scotland (343 FRG), and the British Heart Foundation (PG/11/2/2847) and by a research agreement with Siemens Healthcare.

Conflicts of interest are listed at the end of this article.

See also the editorial by Kramer in this issue.

Radiology 2019; 290:329–337 • https://doi.org/10.1148/radiol.2018181253 • Content code: CA

Purpose: To investigate the prognostic value of circumferential left ventricular (LV) strain measured by using cardiac MRI for prediction of major adverse cardiac events (MACE) following an acute ST-segment–elevation myocardial infarction (STEMI).

Materials and Methods: Participants with acute STEMI were prospectively enrolled from May 11, 2011, to November 22, 2012. Cardiac MRI was performed at 1.5 T during the index hospitalization. Displacement encoding with stimulated echoes (DENSE) and feature tracking of cine cardiac MRI was used to assess circumferential LV strain. MACE that occurred after discharge were independently assessed by cardiologists blinded to the baseline observations.

Results: A total of 259 participants (mean age, 58 years ± 11 [standard deviation]; 198 men [mean age, 58 years ± 11] and 61 women [mean age, 58 years ± 12]) underwent cardiac MRI 2.2 days ± 1.9 after STEMI. Average infarct size was 18% ± 13 of LV mass and circumferential strain was −13% ± 3 (DENSE method) and −24% ± 7 (feature- tracking method). Fifty-one percent (131 of 259 participants) had presence of microvascular obstruction. During a median follow-up period of 4 years, 8% (21 of 259) experienced MACE. Area under the curve (AUC) for DENSE was different from that of feature tracking (AUC, 0.76 vs 0.62; $P = .03$). AUC for DENSE was similar to that of initial infarct size ($P = .06$) and extent of microvascular obstruction ($P = .08$). DENSE-derived strain provided incremental prognostic benefit over infarct size for prediction of MACE (hazard ratio, 1.3; $P < .01$).

Conclusion: Circumferential strain has independent prognostic importance in study participants with acute ST-segment–elevation myocardial infarction.

Online supplemental material is available for this article.

Despite improved early survival after an acute ST-segment–elevation myocardial infarction (STEMI), the incidence of heart failure in the longer term has increased to 32% (1990–1999) from 10% only 20 years earlier (1,2). Standard risk assessment for treatment stratification in individual patients is based on the left ventricular (LV) ejection fraction (LVEF) (3–5) (eg, angiotensin-converting enzyme inhibitor therapy [5,6], implantable defibrillator devices [5,7]). However, this approach has some theoretical limitations because LVEF is only indirectly informative of myocardial contractility. Alternative approaches for estimating the clinical significance of an acute myocardial infarction (MI), such as imaging the size of infarction with cardiac MRI, also has theoretical limitations because the initial size of infarction is overestimated due to edema (8).

Until recently, there was a relative lack of evidence of the utility of cardiac MRI–derived myocardial strain for health outcomes in patients with STEMI (9). In studies of the Abciximab intravenous Versus intracoronary in ST-segment elevation Myocardial Infarction (or AIDA STEMI) population, Eitel et al (10) reported that feature tracking–derived global longitudinal strain but not circumferential strain was an independent risk factor after MI, even after adjusting for LVEF and infarct size. Registry data (11,12) support these findings. Gavara et al (11) reported that feature tracking–derived circumferential strain is a univariable but not a multivariable prognostic indicator for major adverse cardiac events (MACE) in a cohort of 323 patients during 3-year follow-up after MI. Yoon et al (12) reported

Abbreviations

AUC = area under the curve, CI = confidence interval, DENSE = displacement encoding with stimulated echoes, LV = left ventricle, LVEF = LV ejection fraction, MACE = major adverse cardiac events, MI = myocardial infarction, STEMI = ST-segment–elevation MI

Summary

Peak circumferential strain provides prognostic value for major adverse cardiac events over infarct size and characteristics revealed with contrast material–enhanced cardiac MRI.

Implications for Patient Care

- A threshold for circumferential strain of greater than −11% identifies patients at increased risk of major adverse cardiovascular events.
- Strain imaging with displacement encoding with stimulated echoes has emerging potential as a functional imaging marker for prognostication in patients with recent ST-segment–elevation myocardial infarction.

similar findings using feature-tracking software from a different vendor.

Our aim was to investigate circumferential strain in relationship to MACE in study participants with recent STEMI because, theoretically, loss of circumferential myofibers following MI may be particularly deleterious in participants with transmural infarction (13,14). Furthermore, circumferential strain is understudied compared with longitudinal strain in participants after MI (15–17).

Displacement encoding with stimulated echoes (DENSE) (18) encodes myocardial displacement directly into the phase of the cardiac MRI signal allowing for extraction of myocardial strain with pixel-level resolution, conferring a high level of accuracy and reproducibility compared with other methods (18). We hypothesized that DENSE-derived circumferential strain has superior prognostic value when compared with feature tracking of cine imaging.

Our specific hypotheses were to assess the comparative relationships for circumferential strain estimated by using feature-tracking and DENSE methods, LVEF (a reference marker of LV systolic function) (19), initial infarct size (20), and infarct characteristics (microvascular obstruction [21], myocardial salvage index [22]) against MACE.

Materials and Methods

Study Population

A prospective single-center cohort study was performed between May 11, 2011, and November 22, 2012. We enrolled all comers undergoing emergency invasive management for an acute STEMI at a regional cardiac center. Study participants with a contraindication to cardiac MRI were ineligible. The study had ethics approval (reference no. 10-S0703-28) and was publicly registered (clinical trial registration no. NCT 02072850). Written informed consent was secured from each participant.

Siemens Healthcare provided the DENSE work-in-progress cardiac MRI sequence and data analysis software as part of a research agreement with the University of Glasgow. The authors who are not employees of Siemens Healthcare had control of inclusion of any data and information that might present a conflict of interest for those authors who are employees of that industry.

Cardiac MRI Acquisition

Cardiac MRI was performed at 1.5 T (Magnetom Avanto; Siemens Healthcare, Erlangen, Germany) by using an anterior phased-array body coil (12-element) and a posterior phased-array spine coil (24-element) 2 days after MI.

Cardiac MRI Protocol

The cardiac MRI protocol included cine cardiac MRI (balanced steady-state free precession), three short-axis two-dimensional echo-planar imaging DENSE (work-in-progress sequence 611, Siemens Healthcare) (23,24), T2-prepared balanced steady-state free precession sequence, and delayed-enhancement phase-sensitive inversion-recovery pulse sequences (37).

The LV dimensions were assessed by using balanced steady-state free precession cinematographic breath-hold sequences. The heart was imaged in multiple parallel short-axis planes of 7-mm thickness separated by 3-mm gaps. Typical imaging parameters were as follows: 3.3/1.2 (repetition time msec/echo time msec); field of view, 340 mm; flip angle, 80°; spatial resolution, 180 × 256 mm; temporal resolution, 46 msec; bandwidth, 930 Hz/pixel.

T2 maps were acquired in short-axis sections covering the whole ventricle by using a T2-prepared balanced steady-state free precession sequence (work-in-progress sequence 488; Siemens Healthcare) (25). Typical imaging parameters were as follows: bandwidth, 947 Hz/pixel; flip angle, 70°; T2 preparations of 0 msec, 24 msec, and 55 msec, respectively; matrix, 160 × 105 pixels; spatial resolution, 2.6 × 2.1 × 8.0 mm; and section thickness, 8 mm.

Late gadolinium enhancement images covering the entire LV were acquired 10–15 minutes after intravenous injection of 0.15 mmol/kg of gadoterate meglumine (Dotarem; Guebert, France) by using segmented phase-sensitive inversion-recovery turbo fast low-angle shot in a contiguous short-axis LV stack and three orthogonal long-axis planes. Microvascular obstruction was defined as a dark zone at early delayed enhancement imaging 7 minutes after contrast material injection and within an area of late gadolinium enhancement. Typical imaging parameters were as follows: matrix, 192 × 256; flip angle, 25°; echo time, 3.36 msec; bandwidth, 130 Hz/pixel; echo spacing, 8.7 msec; trigger pulse, 2. The voxel size was 1.8 × 1.3 × 8 mm^3. Inversion times were individually adjusted to optimize nulling of visually normal myocardium (typical values, 200 to 300 msec).

Through-plane dephasing and two-point complementary spatial modulation of magnetization were used for artifact suppression during DENSE acquisition (24). Three short-axis sections were acquired (basal, mid-LV, and apical). Fat suppression was carried out by using a fast water excitation option. Readout and phase-encoding direction of displacement were acquired in a single breath hold. Typical DENSE imaging parameters were as follows: 32/8; flip angle, 20°; section thickness, 8 mm; field of view, 360 mm × 270 mm; matrix size, 112 × 84; displacement encoding of 0.2 π/mm; temporal resolution, 55 msec; echo-planar imaging

factor of 8 and segmentation factor of 16; acquisition time of 20 heart beats (Table E1 [online]).

Image Analysis

Image analysis was carried out by using dedicated cardiac MRI software (Argus and Syngo VE32D; Siemens Healthcare) by one author (D.C., a cardiologist with >3 years of MRI experience) and reviewed by another author (C.B., a cardiologist with >10 years of MRI experience). Image analysis was typically conducted within 2 weeks of acquisition. The extent of myocardial edema was defined as the amount of LV myocardium with pixel values (T2, msec) greater than 2 standard deviations from remote myocardium and expressed as percentage of LV mass. Late gadolinium enhancement was quantified by using computer-assisted planimetry with the 5 standard deviation technique and expressed as percentage of LV mass. Microvascular obstruction was defined as a dark zone within areas of late gadolinium enhancement obtained 10–15 minutes after intravenous administration and expressed as percentage of LV mass (26).

DENSE was analyzed by using CIM_DENSE2D software (University of Auckland, New Zealand) (27). Circumferential strain was determined on basal, mid-LV, and apical DENSE images; all levels were averaged to determine global circumferential strain. Cardiac MRI feature-tracking software (Diogenes; TomTec Imaging Systems, Munich, Germany) was used to quantify strain from basal, mid-LV, and apical short-axis cine imaging spatially coregistered to the DENSE images. The same operator (K.M.) derived strain following a standard protocol taught by the software manufacturer (28). All levels were averaged to determine global circumferential strain. We did not assess wall motion scores because these are no longer cited in clinical guidelines (5).

Myocardial salvage was calculated by subtraction of percent infarct size from percent area at risk. The myocardial salvage index was calculated by dividing the myocardial salvage area by the initial area at risk.

All data were analyzed from data sets in a random order. The image analysts were blinded to participant demographics and clinical outcomes. DENSE and cine image quality and artifact scoring were carried out by two operators in consensus (K.M., a cardiologist with >3 years of cardiac MRI experience; C.M., a MRI scientist with >10 years of cardiac MRI experience), and a third expert observer (X.Z., a MRI scientist with >10 years of cardiac MRI experience) acted as a blinded independent adjudicator. A Likert scoring system was used to report image quality. Imaging data sets for DENSE and feature tracking (n = 20) were reanalyzed 2 weeks later in random order for intraobserver (K.M.) and interobserver (C.M.) variability.

Health Outcomes

Adverse health outcomes that are pathophysiologically linked with STEMI were prespecified (29). The primary composite outcome was spontaneous MACE defined as cardiac death, nonfatal myocardial infarction, or hospitalization for heart failure. Only serious adverse events arising after the index hospitalization (ie, after discharge) were evaluated.

Research team members (J.C., a physician) screened for adverse events through national electronic medical records of the study participants and by contacting participants and their primary and secondary care physicians, as appropriate. Each event was reviewed by a cardiologist independent of the research team and blinded to all the clinical and cardiac MRI data (A.M., a cardiologist). The adverse events were defined according to standard guidelines (29) and categorized as having occurred during the index admission or postdischarge.

Statistical Analysis

Statistical analysis was performed by using R (version 2.15 or higher; R Foundation for Statistical Computing, Vienna, Austria; *https://www.r-project.org*) under supervision of a biostatistician (C.H.). Normality was tested by using box plots. Continuous variables were expressed as means ± standard deviations or medians and interquartile ranges (Q1, Q3), depending on distribution. Skewed distributions were analyzed by using Mann-Whitney or Kruskal-Wallis tests. A P value of $< .05$ was considered to indicate statistical significance. Multivariable logistic regression models were constructed to assess the incremental prognostic utility of parameters over infarct size for MACE.

Receiver operating characteristic, Cox proportional hazards regression, and Kaplan-Meier curves were used to identify potential predictors of MACE. The proportional hazards assumption was tested by using log-minus-log plots. Diagnostic cutoff values were identified from the "Optimal Cutpoints" package (30) by using the Youden index (31). Log-rank analysis was carried out to identify whether the cutoff value identified for these predictors was statistically significant. The difference in area under the curve (AUC) was compared by using the z statistic. The sample size calculation can be found in Appendix E1 (online).

Results

Characteristics of the Study Participants

A total of 300 of 343 screened participants referred for emergency percutaneous coronary intervention underwent 1.5-T cardiac MRI 2.2 days ± 1.9 (standard deviation) after hospital admission (Fig 1). Among the 300 study participants, 261 (87%) underwent DENSE imaging, whereas all participants (100%) underwent cine imaging. Thirty-nine (13%) participants did not undergo DENSE imaging, either because the method was unavailable (15 of 300, 5%) or because of intolerance of the cardiac MRI examination (24 of 300, 8%) (Fig 1). The mean age for male participants (198 of 259, 76%) was 58 years ± 11 (range, 33–83 years) and that for female participants (61 of 259, 24%) was 58 years ± 12 (range, 32–85 years). The characteristics of the participants with DENSE imaging findings are described in Table 1. The cardiac MRI findings for participants are described in Table 2, and clinical examples are illustrated in Figure 2.

DENSE Image Quality

Image quality was high or adequate in the majority of DENSE and feature-tracking acquisitions for circumferential strain (Table E2 [online]). Fourteen of 783 (1.8%) DENSE myocardial seg-

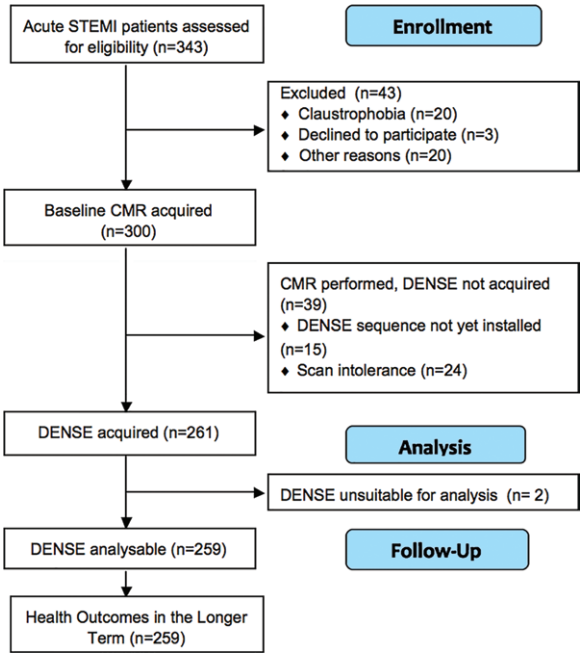

Figure 1: Consolidated Standards of Reporting Trials, or CONSORT, study diagram. CMR = cardiac MRI, DENSE = displacement encoding with stimulated echoes, STEMI = ST-segment–elevation myocardial infarction.

ments were nondiagnostic. Two participants underwent nondiagnostic DENSE imaging. All of the cine images were diagnostic. The intraclass correlation coefficient was excellent (>0.90) for all intraobserver and interobserver analyses. The mean bias between attempts or operators was not clinically significant at 1% (Table E3 [online]).

Prognostic Value of Cardiac MRI Parameters

The median follow-up duration was 4 years (median, 1501 days; range, 1241–1802 days). Follow-up was achieved in all (259 of 259, 100%) study participants. Among 259 participants, 21 participants (8%) experienced spontaneous MACE after discharge from their index admission. The associations of global circumferential strain, LVEF, initial infarct size, and myocardial salvage index in relationship to MACE were assessed by using receiver operating characteristic analysis. The optimal cutoffs for MACE for all the baseline variables were identified by using the Youden index (31) (Table 3).

The AUC of circumferential strain with DENSE to predict MACE was 0.76. Initial infarct size (AUC, 0.67), microvascular obstruction extent (AUC, 0.63), and feature tracking (AUC, 0.62) had similar AUC values to predict MACE. AUC for DENSE was different from that of feature tracking (*z* statistic, 2.2; $P = .03$), whereas it was not different from initial infarct size (*z* statistic, 1.8; $P = .06$) or extent of microvascular obstruction (*z* statistic, 1.7; $P = .08$). LVEF (AUC, 0.35; $P = .03$) and myocardial salvage index (AUC, 0.34; $P = .02$) were classified as "below chance" to predict MACE.

The optimal discriminative cutoffs for MACE were greater than or equal to −11% for circumferential strain with DENSE, greater than or equal to −19% for feature tracking, greater than or equal to 32% for initial infarct size (percentage of LV mass), and greater than or equal to 7.8% for microvascular obstruction (percentage of LV mass). By using Kaplan-Meier survival analysis and log-rank testing, the variables with discriminative potential were as follows: DENSE ($\chi^2 = 19$; $P < .001$), microvascular obstruction ($\chi^2 = 13$; $P < .001$), infarct size ($\chi^2 = 9.4$; $P = .002$), and feature tracking ($\chi^2 = 5.2$; $P = .02$) (Table 3, Figures 3–6).

Incremental Prognostic Utility of Strain over Infarct Size for Health Outcomes

A multivariable Cox proportional hazards regression model was used to assess whether baseline parameters provided incremental prognostic benefit over initial infarct size for MACE.

Circumferential strain with DENSE was associated with incremental prognostic value over baseline infarct size for prediction of MACE (hazard ratio, 1.26; 95% confidence interval [CI]: 1.09, 1.46; $P = .002$) (Table 4), whereas LVEF (hazard ratio, 0.98; 95% CI: 0.92, 1.04; $P = .44$), microvascular obstruction (hazard ratio, 1.02; 95% CI: 0.94, 1.11; $P = .61$), myocardial salvage index (hazard ratio, 0.99; 95% CI: 0.96, 1.01; $P = .11$), and circumferential strain with feature tracking (hazard ratio, 1.03; 95% CI: 0.94, 1.12; $P = .54$) had no incremental prognostic value.

Discussion

We investigated the comparative prognostic utility of circumferential strain revealed with cardiac MRI in a reasonably large and unselected population of participants with STEMI per complete follow-up during a 4-year period. Our main findings are as follows: First, feature tracking was feasible in all the participants. DENSE was feasible and informative in the majority of participants. Second, circumferential strain with DENSE has incremental prognostic value over initial infarct size for the future occurrence of MACE during a median of 4-year follow-up after the index hospitalization. Finally, a circumferential strain threshold of −11% with DENSE has higher predictive value than does initial infarct size threshold of 32% of LV mass to identify participants at higher risk of MACE. Strain imaging with DENSE has emerging potential as reference functional biomarker for prognostication in patients after an acute STEMI.

Circumferential Strain

Strain imaging is increasingly adopted for clinical and research purposes in patients following MI, representing an advance on historical approaches, such as wall motion scoring (5). Our results indicate that loss of circumferential strain with DENSE has clinically significant implications in patients following MI, while obviating contrast. DENSE resolves circumferential strain with high precision and accuracy (23,24). LV pump function (or pump failure) is a critical determinant of heart failure after MI. Longitudinal myofibers are distributed within the subendocardium of the heart. Given the endo-epicardial wave-front of ischemia (32), these fibers are anatomically predisposed to infarction. Circumferential myofibers are located within the midwall and epicardium and are therefore less susceptible to ischemia and subsequent in-

Table 1: Demographics of Participants with Acute STEMI

Characteristic	All Participants (n = 259)	No MACE (n = 238)	MACE (n = 21)	P Value
Age (y)*	58 ± 11	58 ± 11	54 ± 7	.08
Sex				.57
Male	198 (76)	183	15	
Female	61 (24)	55	6	
Weight (kg)*	82 ± 15	82 ± 15	81 ± 14	.73
Body mass index (kg/m^2)*	29 ± 5	29 ± 5	29 ± 5	.41
Hypertension	78 (30)	71	7	.73
Current smoker	159 (61)	142	16	.14
Hypercholesterolemia	70 (27)	7	62	.45
Diabetes mellitus†	27 (10)	4	23	.18
Presenting characteristics*				
Heart rate (bpm)	77 ± 17	77 ± 17	83 ± 15	.10
Systolic blood pressure (mm Hg)	136 ± 25	135 ± 24	148 ± 29	.03
Time from symptom onset to reperfusion (min)	251 ± 200	247 ± 191	287 ± 281	.39
No. of diseased arteries‡				
One	147 (57)	136	10	…
Two	78 (30)	69	8	.63
Three	34 (13)	28	3	…
Anterior infarction	97 (37)	12	85	.14
TIMI coronary flow grade before PCI				
0/1	193 (75)	174	20	…
2	44 (17)	44	0	.14
3	22 (8)	20	1	…
TIMI coronary flow grade after PCI				
0/1	4 (2)	4	0	…
2	8 (3)	8	1	.46
3	247 (95)	226	20	…

Note.—Unless otherwise specified, data are the number of participants, with percentages in parentheses. MACE = major adverse cardiac events, PCI = percutaneous coronary intervention, STEMI = ST-segment–elevation myocardial infarction, TIMI = thrombolysis in myocardial infarction.

* Data are means ± standard deviations.

† Diabetes mellitus was defined as a history of diet-controlled or treated diabetes.

‡ Multivessel coronary artery disease was defined according to the number of stenoses of at least 50% of the reference vessel diameter by using visual assessment.

Table 2: Cardiac MRI Characteristics for the Study Population

Parameter	All Participants (n = 259)	No MACE (n = 238)	MACE (n = 21)	P Value
LV ejection fraction (%)*	56 ± 10	55 ± 9	50 ± 12	.02
LVEDVi (mL/m^2)	79 (26, 44)	79 (69, 86)	90 (74, 101)	.02
LVESVi (mL/m^2)	35 (26, 44)	35 (25, 43)	44 (32, 54)	.01
Circumferential strain*				
DENSE (%)	−13 ± 3	−14 ± 3	−11 ± 3	<.01
Feature tracking (%)	−24 ± 7	−24 ± 6	−21 ± 8	.04
Myocardial salvage index (%)	60 (43, 84)	61 (44, 86)	43 (31, 64)	.02
Infarct size†	16 (7, 27)	15 (6,26)	22 (14, 39)	.01
Microvascular obstruction†	0 (0, 3)	0 (0, 3)	1 (0, 11)	.04

Note.—Unless otherwise specified, data are medians with interquartile ranges in parentheses. DENSE = displacement encoding with stimulated echoes, LV = left ventricle, LVEDVi = LV end-diastolic volume indexed to body surface area, LVESVi = LV end-systolic volume indexed to body surface area, MACE = major adverse cardiac events.

* Data are means ± standard deviations.

† Assessed as the percentage of LV mass.

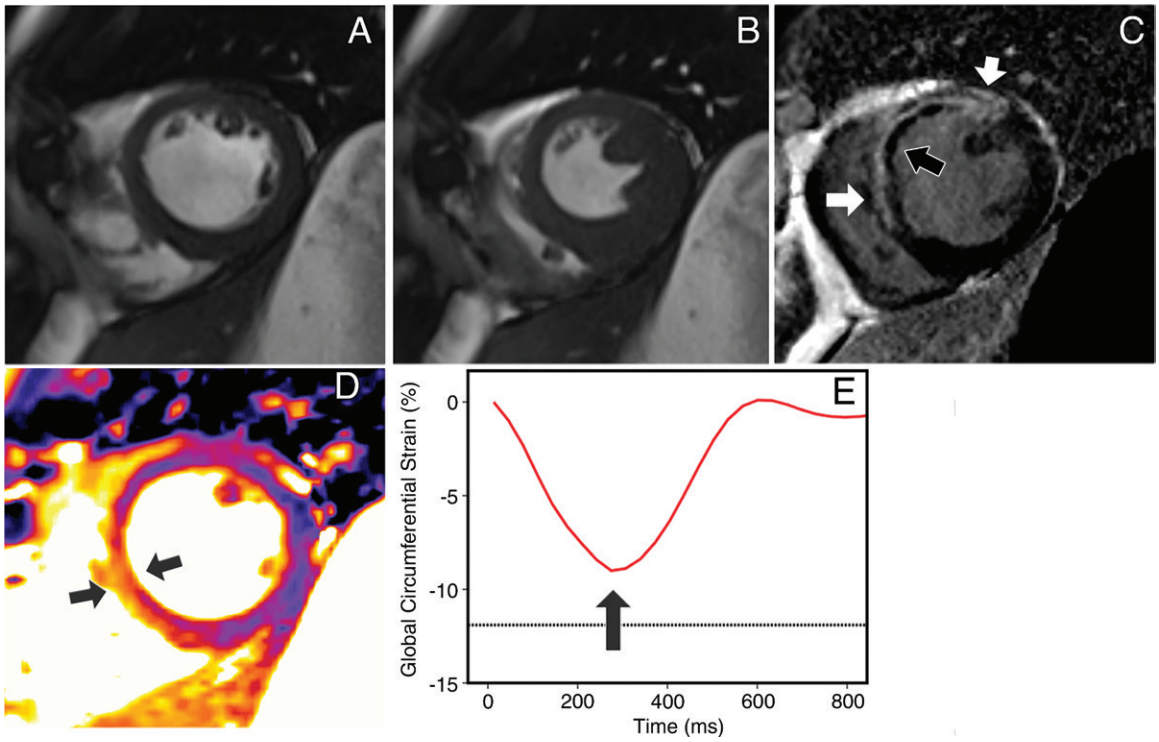

Figure 2: Images demonstrate strain and adverse health outcomes in a 61-year-old man who presented with acute anterior ST-segment–elevation myocardial infarction (STEMI). Coronary angiography revealed occluded left anterior descending artery. Cardiac MRI at day 2 after STEMI revealed anteroseptal wall motion abnormality. *A*, Cine image at midventricular level in, *B*, end-diastole during midsystole. *C*, Late gadolinium enhancement imaging at same midventricular level shows left ventricle (LV) ejection fraction of 45%, infarct size (white arrows) of 43% of LV mass, and extent of microvascular obstruction (black arrow) of 12% of LV mass. *D*, T2 mapping was used to calculate myocardial salvage index of 31%; arrows indicate edema. *E*, Graph shows peak global circumferential strain with displacement encoding with stimulated echoes of −9% (arrow). This patient presented acutely to hospital with heart failure at 6 months after discharge.

Table 3: Cutoffs for Prediction of MACE in 259 Patients

Parameter	AUC*	Cutoff Value†	*Z* Statistic	*P* Value‡	Sensitivity (%)§	Specificity (%)§	Kaplan-Meier Survival Analyses (χ^2)	Log-Rank *P* Value
LV ejection fraction (%)	0.36 (0.23, 0.49)	71	NA	…	10 (2/21)	96 (228/238)	0.02	.89
Myocardial salvage index (%)	0.34 (0.22, 0.46)	28	NA	…	94 (19/21)	11 (26/238)	0.01	.97
Infarct size‖	0.67 (0.54, 0.81)	32	1.8	.06	43 (9/21)	89 (211/238)	9.4	<.01
Microvascular obstruction‖	0.63 (0.48, 0.78)	7.8	1.7	.08	43 (9/21)	89 (212/238)	13	<.01
Global circumferential strain (%)								
DENSE	0.76 (0.64, 0.87)	−11	Reference	…	67 (14/21)	79 (188/238)	19	<.01
Feature tracking	0.62 (0.47, 0.76)	−19	2.2	.03	47 (9/21)	79 (188/238)	5.2	.02

Note.— There were 21 patients with major adverse cardiac events (MACE) and 238 patients with no MACE. AUC = area under the curve, DENSE = displacement encoding with stimulated echoes, LV = left ventricle, NA = not applicable.

* Data in parentheses are 95% confidence intervals.

† Cutoffs were derived from the same data set, not from a validation data set, and may overestimate performance.

‡ Compared with DENSE.

§ Data in parentheses are numerators and denominators.

‖ Assessed as the percentage of LV mass.

farction based on anatomic location. Circumferential strain may therefore represent a functional biomarker of myocardial salvage and the propensity to recovery of LV pump function in the longer term. Loss of circumferential strain early after MI would then become more important (33).

Our findings are consistent with those of two studies (11,12) that reported feature tracking–derived circumferential strain as a univariable but not a multivariable predictor of MACE. As in our own study, both had comparatively long follow-up durations (median of 3.0 years [11] and 7.8 years [12], respectively).

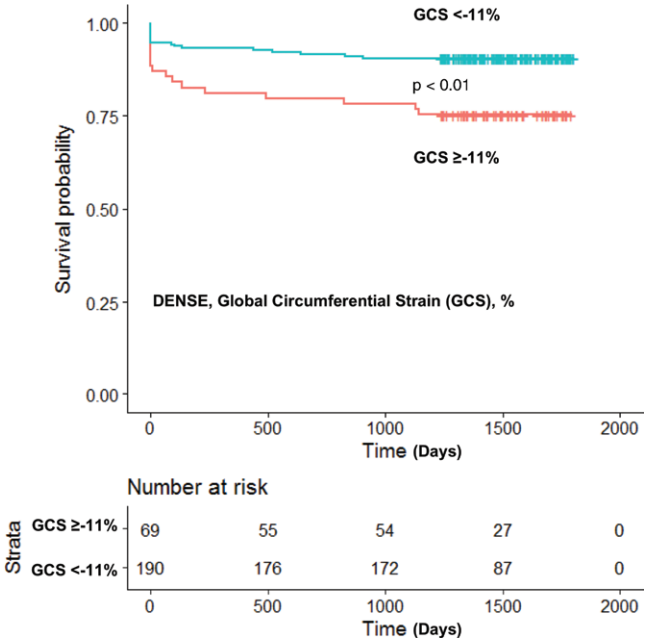

Figure 3: Graphs show Kaplan-Meier survival curves for 259 participants with ST-segment–elevation myocardial infarction grouped by displacement encoding with stimulated echoes (DENSE)–derived strain and major adverse cardiac events (n = 21) after discharge from hospital during follow-up over 4 years.

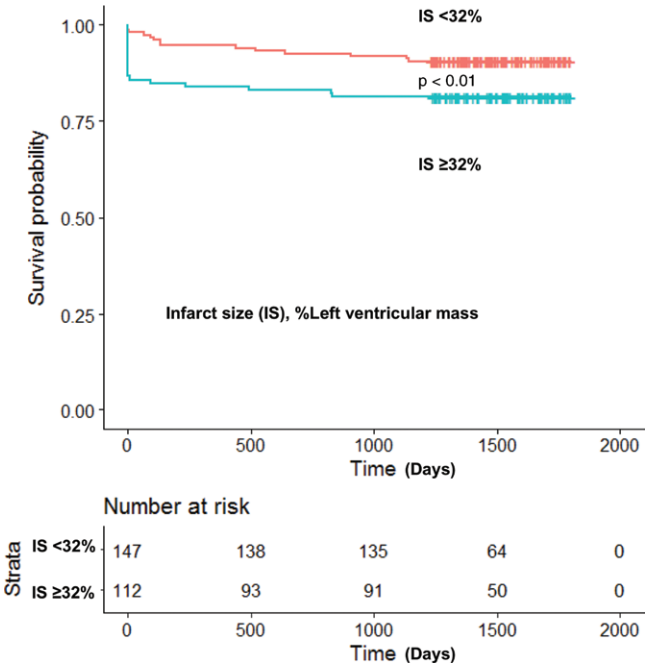

Figure 5: Graphs show Kaplan-Meier survival curves for 259 participants with ST-segment–elevation myocardial infarction grouped by initial infarct size and major adverse cardiac events (n = 21) after discharge from hospital to 4-year follow-up.

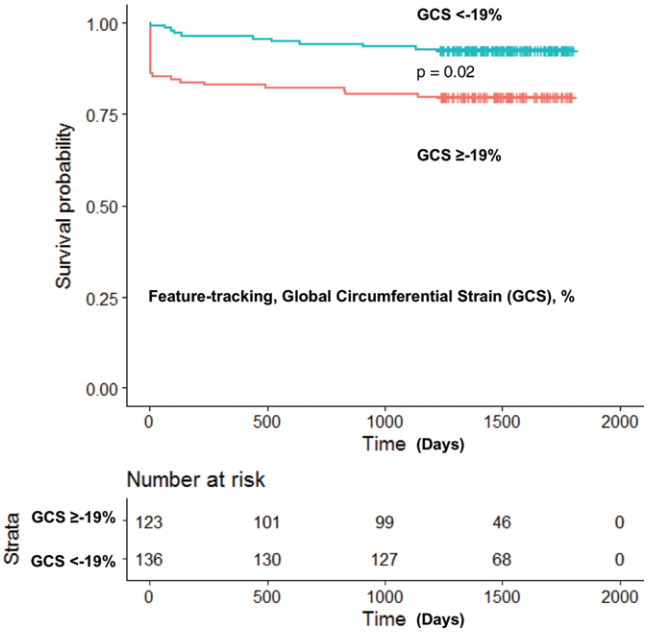

Figure 4: Graphs show Kaplan-Meier survival curves for 259 participants with ST-segment–elevation myocardial infarction grouped by feature tracking–derived strain and major adverse cardiac events (n = 21) after discharge from hospital to 4-year follow-up.

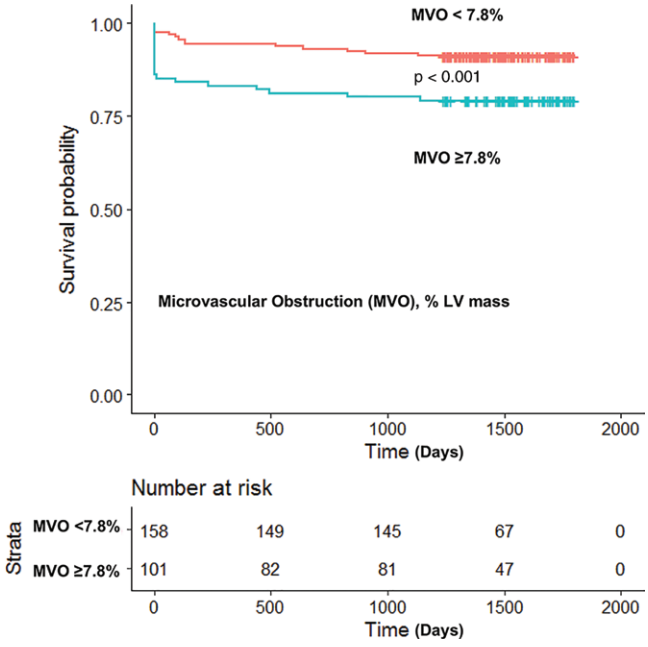

Figure 6: Graphs show Kaplan-Meier survival curves for 259 participants with ST-segment–elevation myocardial infarction grouped by extent of late microvascular obstruction and major adverse cardiac events (n = 21) after discharge from hospital to 4-year follow-up. LV = left ventricle.

In a landmark study investigating the prognostic value of feature tracking–derived strain pooled from clinical trials, Eitel et al (10) identified feature-tracking longitudinal and circumferential strain as univariable predictors of MACE. The timing of cardiac MRI in these studies ranged from 1–10 days after MI (34). This time interval is comparatively long, which is especially relevant for LV dimensions and microvascular obstruction that change dynamically within the first 48 hours after MI (35). The other two studies are retrospective in nature; selected from cardiac MRI registries in which patients after STEMI were referred for a cardiac MRI, possibly resulting in selection bias. In the study by Yoon et al (12), the time range for cardiac MRI was 1–30 days after MI. In the study

Table 4: Incremental Prognostic Benefit of Circumferential Strain over Baseline Infarct Size for Composite Health Outcomes

Analysis	Hazard Ratio*	*P* Value
Univariable analysis		
Initial infarct size†	1.04 (1.01, 1.07)	.01
Global circumferential strain (%)		
DENSE	1.26 (1.12, 1.48)	<.01
Feature tracking	1.07 (1.00, 1.15)	.04
LV ejection fraction at baseline (%)	0.95 (0.91, 0.99)	.02
Myocardial salvage index	0.98 (0.96, 1.00)	.02
Microvascular obstruction†	1.07 (1.02, 1.14)	.01
Multivariable analysis		
Model 1, infarct size + DENSE		
Initial infarct size†	1.01 (0.98, 1.04)	.44
DENSE, E_{CC} (%)	1.26 (1.09, 1.46)	.002
Model 2, infarct size + feature tracking		
Initial infarct size†	1.03 (1.00, 1.07)	.10
Feature tracking, E_{CC} (%)	1.03 (0.94, 1.12)	.54
Model 3, infarct size + LV ejection fraction		
Initial infarct size†	1.03 (0.99, 1.07)	.15
LV ejection fraction at baseline (%)	0.98 (0.92, 1.04)	.44
Model 4, infarct size + myocardial salvage index		
Initial infarct size†	1.03 (0.99, 1.08)	.11
Myocardial salvage index	0.99 (0.96, 1.01)	.11
Model 5, infarct size + microvascular obstruction		
Initial infarct size†	1.03 (0.99, 1.08)	.13
Microvascular obstruction†	1.02 (0.94, 1.11)	.61

Note.—DENSE = displacement encoding with stimulated echoes, E_{CC} = global circumferential strain, LV = left ventricle, MACE = major adverse cardiac events.

* Data in parentheses are 95% confidence intervals.

† Assessed as the percentage of LV mass.

by Gavara et al (11), cardiac MRI was performed on average 7 days after STEMI. In this study, global circumferential strain was a univariable but not a multivariable predictor of MACE.

Considering the overall number of MACE, the number of in-hospital MACE (34 of 259, 14%) was comparably high. Because only those MACE that occur after the initial cardiac MRI should be counted for risk prediction, we restricted the health outcomes analysis to include only events that occurred after discharge. We adopted this stringent approach to rule out the possibility of overlap between MACE that may be closely associated with the timing of cardiac MRI in-hospital. Furthermore, MACE in this analysis were spontaneous and, in line with regulatory guidelines (29), did not include revascularizations. The rate of MACE after discharge (8%) reflects the fact that in-hospital MACE and revascularizations were not included, as has been the case in other imaging cohort studies (22,36).

Infarct Size, Microvascular Obstruction

We also studied the comparative prognostic value of infarct size versus LVEF after MI. A patient-level analysis of 2632 participants with infarct size assessed by using contrast material–enhanced cardiac MRI or technetium 99m sestamibi single-photon emission CT found that infarct size measured within 1 month of the initial presentation was strongly associated with all-cause mortality and hospitalization for heart failure within 1 year (20). Our results extend the evidence on the prognostic importance of infarct size in the longer term (4 years) and lend further support to the value of infarct size as a more informative surrogate for therapeutic efficacy than LVEF. We found that an infarct size of greater than or equal to 32% of LV mass represents a threshold for MACE in the longer term.

Unlike the meta-analysis of 1025 patients presented by van Kranenberg et al (21), microvascular obstruction did not provide incremental prognostic benefit over infarct size in our study. This is most likely due to the number of events in our study (n = 21; 8%) compared with the meta-analysis (n = 130; 13%). There are a number of potential explanations. Our number of events is numerically smaller. Microvascular obstruction only occurs in a subset of patients (ie, half of patients are affected). Furthermore, the extent of microvascular obstruction and infarct size are highly correlated (21).

Our study had some limitations. We do not have information on longitudinal strain by using cardiac MRI or echocardiography. We performed a single-center study and further research is warranted. The number of MACE was low (21 of 259, 8%), which restricts variable use in multivariable regression analysis. We did not use an independent validation set of participants with STEMI, and thus these cutoffs would overestimate performance. We used a work-in-progress echo-planar imaging DENSE method. Spiral cine MRI with DENSE is now available. Because this method may have enhanced diagnostic performance, further studies seem warranted.

In conclusion, peak circumferential strain with displacement encoding with stimulated echoes MRI provides incremental prognostic value over infarct size and pathologies revealed with contrast-enhanced cardiac MRI for major adverse cardiac events.

Acknowledgments: The authors thank the patients and the staff in the Cardiology and Radiology departments.

Author contributions: Guarantors of integrity of entire study, H.E., C.B.; study concepts/study design or data acquisition or data analysis/interpretation, all authors; manuscript drafting or manuscript revision for important intellectual content, all authors; approval of final version of submitted manuscript, all authors; agrees to ensure any questions related to the work are appropriately resolved, all authors; literature research, K.M., D.C., H.E., M.C.P., F.H.E., C.B.; clinical studies, K.M., D.C., A.M., C.M., K.G.O., H.E., M.L., M.M., S.H., M.C.P., A.D., X.Z., C.B.; statistical analysis, K.M., J.C., H.E., C.E.H.; and manuscript editing, K.M., D.C., A.M., C.M., K.G.O., H.E., M.L., M.M., M.C.P., X.Z., F.H.E., C.E.H., C.B.

Disclosures of Conflicts of Interest: **K.M.** disclosed no relevant relationships. **D.C.** disclosed no relevant relationships. **J.C.** disclosed no relevant relationships. **A.M.** disclosed no relevant relationships. **C.M.** disclosed no relevant relationships. **K.G.O.** disclosed no relevant relationships. **H.E.** disclosed no relevant relationships. **M.L.** disclosed no relevant relationships. **M.M.** disclosed no relevant relationships. **S.H.** disclosed no relevant relationships. **M.C.P.** disclosed no relevant relationships. **S.W.** disclosed no relevant relationships. **A.D.** disclosed no relevant relationships. **X.Z.** Activities related to the present article: disclosed no relevant relationships. Activities not related to the present article: is an employee of Siemens. Other relationships: author holds several pending patents jointly owned by Siemens and/or Emory University and University of Virginia about topics related to displacement encoding with stimulated echoes (DENSE) technique; author received incentives from Siemens; institutions may receive income from the pending patents. **F.H.E.** Activities related to the present article: institution received payment for grant from Siemens. Activities not related to the present article: disclosed no relevant relationships. Other relationships: institution received payment for grant no. US7813537B2 for motion-guided segmentation for cine DENSE images. **C.E.H.** disclosed no relevant relationships. **C.B.** Activities related to the present article: disclosed no relevant relationships. Activities not related to the present article: institution received payment for travel/accommodations/meeting expenses unrelated to activities listed from Philips. Other relationships: disclosed no relevant relationships.

References

1. Velagaleti RS, Pencina MJ, Murabito JM, et al. Long-term trends in the incidence of heart failure after myocardial infarction. Circulation 2008; 118(20):2057–2062.
2. Gerber Y, Weston SA, Enriquez-Sarano M, et al. Mortality associated with heart failure after myocardial infarction: a contemporary community perspective. Circ Heart Fail 2016;9(1):e002460.
3. White HD, Norris RM, Brown MA, Brandt PW, Whitlock RM, Wild CJ. Left ventricular end-systolic volume as the major determinant of survival after recovery from myocardial infarction. Circulation 1987;76(1):44–51.
4. O'Gara PT, Kushner FG, Ascheim DD, et al. 2013 ACCF/AHA guideline for the management of ST-elevation myocardial infarction: executive summary: a report of the American College of Cardiology Foundation/American Heart Association Task Force on Practice Guidelines: developed in collaboration with the American College of Emergency Physicians and Society for Cardiovascular Angiography and Interventions. Catheter Cardiovasc Interv 2013;82(1):E1–E27.
5. Ibanez B, James S, Agewall S, et al. 2017 ESC guidelines for the management of acute myocardial infarction in patients presenting with ST-segment elevation: the Task Force for the management of acute myocardial infarction in patients presenting with ST-segment elevation of the European Society of Cardiology (ESC). Eur Heart J 2018;39(2):119–177.
6. St John Sutton M, Pfeffer MA, Moye L, et al. Cardiovascular death and left ventricular remodeling two years after myocardial infarction: baseline predictors and impact of long-term use of captopril: information from the Survival and Ventricular Enlargement (SAVE) trial. Circulation 1997;96(10):3294–3299.
7. Lee DS, Green LD, Liu PP, et al. Effectiveness of implantable defibrillators for preventing arrhythmic events and death: a meta-analysis. J Am Coll Cardiol 2003;41(9):1573–1582.
8. Dall'Armellina E, Karia N, Lindsay AC, et al. Dynamic changes of edema and late gadolinium enhancement after acute myocardial infarction and their relationship to functional recovery and salvage index. Circ Cardiovasc Imaging 2011;4(3):228–236.
9. Mangion K, McComb C, Auger DA, Epstein FH, Berry C. Magnetic resonance imaging of myocardial strain after acute ST-segment-elevation myocardial infarction: a systematic review. Circ Cardiovasc Imaging 2017;10(8):e006498.
10. Eitel I, Stiermaier T, Lange T, et al. Cardiac magnetic resonance myocardial feature tracking for optimized prediction of cardiovascular events following myocardial infarction. JACC Cardiovasc Imaging 2018 Feb 9. pii: S1936-878X(17)31176-2 [Epub ahead of print].
11. Gavara J, Rodriguez-Palomares JF, Valente F, et al. Prognostic value of strain by tissue tracking cardiac magnetic resonance after ST-segment elevation myocardial infarction. JACC Cardiovasc Imaging 2017 Dec 8. pii: S1936-878X(17)30985-3 [Epub ahead of print].
12. Yoon YE, Kang SH, Choi HM, et al. Prediction of infarct size and adverse cardiac outcomes by tissue tracking-cardiac magnetic resonance imaging in ST-segment elevation myocardial infarction. Eur Radiol 2018;28(8):3454–3463.
13. Kramer CM, Rogers WJ, Theobald TM, Power TP, Petruolo S, Reichek N. Remote noninfarcted region dysfunction soon after first anterior myocardial infarction: a magnetic resonance tagging study. Circulation 1996;94(4): 660–666.
14. Caracciolo G, Eleid MF, Abe H, et al. Non-uniform recovery of left ventricular transmural mechanics in ST-segment elevation myocardial infarction. Cardiovasc Ultrasound 2010;8(1):31.
15. Ersbøll M, Valeur N, Mogensen UM, et al. Prediction of all-cause mortality and heart failure admissions from global left ventricular longitudinal strain in patients with acute myocardial infarction and preserved left ventricular ejection fraction. J Am Coll Cardiol 2013;61(23):2365–2373.
16. Munk K, Andersen NH, Terkelsen CJ, et al. Global left ventricular longitudinal systolic strain for early risk assessment in patients with acute myocardial infarction treated with primary percutaneous intervention. J Am Soc Echocardiogr 2012;25(6):644–651.
17. Hung CL, Verma A, Uno H, et al. Longitudinal and circumferential strain rate, left ventricular remodeling, and prognosis after myocardial infarction. J Am Coll Cardiol 2010;56(22):1812–1822.
18. Aletras AH, Ding S, Balaban RS, Wen H. DENSE: displacement encoding with stimulated echoes in cardiac functional MRI. J Magn Reson 1999;137(1):247–252.
19. Kelly MJ, Thompson PL, Quinlan MF. Prognostic significance of left ventricular ejection fraction after acute myocardial infarction: a bedside radionuclide study. Br Heart J 1985;53(1):16–24.
20. Stone GW, Selker HP, Thiele H, et al. Relationship between infarct size and outcomes following primary PCI: patient-level analysis from 10 randomized trials. J Am Coll Cardiol 2016;67(14):1674–1683.
21. van Kranenburg M, Magro M, Thiele H, et al. Prognostic value of microvascular obstruction and infarct size, as measured by CMR in STEMI patients. JACC Cardiovasc Imaging 2014;7(9):930–939.
22. Eitel I, Desch S, Fuernau G, et al. Prognostic significance and determinants of myocardial salvage assessed by cardiovascular magnetic resonance in acute reperfused myocardial infarction. J Am Coll Cardiol 2010;55(22):2470–2479.
23. Kim D, Gilson WD, Kramer CM, Epstein FH. Myocardial tissue tracking with two-dimensional cine displacement-encoded MR imaging: development and initial evaluation. Radiology 2004;230(3):862–871.
24. Zhong X, Spottiswoode BS, Cowart EA, Gilson WD, Epstein FH. Selective suppression of artifact-generating echoes in cine DENSE using through-plane dephasing. Magn Reson Med 2006;56(5):1126–1131.
25. Giri S, Chung YC, Merchant A, et al. T2 quantification for improved detection of myocardial edema. J Cardiovasc Magn Reson 2009; 11(1):56.
26. Carrick D, Haig C, Rauhalammi S, et al. Pathophysiology of LV remodeling in survivors of STEMI: inflammation, remote myocardium, and prognosis. JACC Cardiovasc Imaging 2015;8(7):779–789.
27. Young AA, Li B, Kirton RS, Cowan BR. Generalized spatiotemporal myocardial strain analysis for DENSE and SPAMM imaging. Magn Reson Med 2012;67(6):1590–1599.
28. Hor KN, Gottliebson WM, Carson C, et al. Comparison of magnetic resonance feature tracking for strain calculation with harmonic phase imaging analysis. JACC Cardiovasc Imaging 2010;3(2):144–151.
29. Hicks KA, Tcheng JE, Bozkurt B, et al. 2014 ACC/AHA key data elements and definitions for cardiovascular endpoint events in clinical trials: a report of the American College of Cardiology/American Heart Association Task Force on clinical data standards (writing committee to develop cardiovascular endpoints data standards). Circulation 2015;132(4):302–361.
30. López-Ratón M, Rodríguez-Álvarez MX, Suarez CC, Sampedro FG. OptimalCutpoints: an R package for selecting optimal cutpoints in diagnostic tests. J Stat Softw 2014;61(8):1–36.
31. Youden WJ. Index for rating diagnostic tests. Cancer 1950;3(1):32–35.
32. Kloner RA, Ganote CE, Jennings RB. The "no-reflow" phenomenon after temporary coronary occlusion in the dog. J Clin Invest 1974;54(6):1496–1508.
33. Bogaert J, Bosmans H, Maes A, Suetens P, Marchal G, Rademakers FE. Remote myocardial dysfunction after acute anterior myocardial infarction: impact of left ventricular shape on regional function: a magnetic resonance myocardial tagging study. J Am Coll Cardiol 2000;35(6):1525–1534.
34. Bulluck H, Hammond-Haley M, Weinmann S, Martinez-Macias R, Hausenloy DJ. Myocardial infarct Size by CMR in clinical cardioprotection studies: insights from randomized controlled trials. JACC Cardiovasc Imaging 2017;10(3):230–240.
35. Carrick D, Haig C, Ahmed N, et al. Temporal evolution of myocardial hemorrhage and edema in patients after acute ST-segment elevation myocardial infarction: pathophysiological insights and clinical implications. J Am Heart Assoc 2016 Feb 23;5(2). pii: e002834.
36. Kelle S, Roes SD, Klein C, et al. Prognostic value of myocardial infarct size and contractile reserve using magnetic resonance imaging. J Am Coll Cardiol 2009;54(19):1770–1777.
37. Kellman P, Arai AE, McVeigh ER, Aletras AH. Phase-sensitive inversion recovery for detecting myocardial infarction using gadolinium-delayed hyperenhancement. Magn Reson Med 2002;47(2):372–383.